Fluid Dynamics — Numerical Techniques

MATH5453M Numerical Exercises 2, 2024

Due date: November 15th 2024

Leading-order DGFEM0 or Godunov method

Finite Volume Method: linear shallow-water equations, predicting surf height at beaches

Consider the linearised shallow-water system of equations

$$\frac{\partial \eta}{\partial t} + \frac{\partial (Hu)}{\partial x} = 0 \quad \text{and} \quad \frac{\partial u}{\partial t} + \frac{\partial (g\eta)}{\partial x} = 0 \tag{1}$$

for the variables velocity $u = u(x,t)$ and free-surface deviation $\eta = \eta(x,t)$, rest depth $H(x)$ and acceleration of gravity $g = 9.81\text{m/s}^2$. When we scale (1) as follows

$$u = U_0 u', \quad x = L_s x', \quad t = (L_s/U_0)t', \quad \eta = H_{0s}\eta', \quad H = H_{0s}H' \tag{2}$$

with primed dimensionless variables then g can be replaced by a dimensionless $g' = gH_{0s}/U_0^2$ and we can work with scaled equations. (Show this.) These latter, scaled equations look exactly the same as (1), when we drop the primes, but g' (or g once primes are dropped) can attain different (dimensionless) values depending on the choices of L_s, H_{0s} and U_{0s}; furthermore, when $U_0^2 = gH_{0s}$ we note that $g' = 1$. We usually drop the primes after the scaling.

1. Define the Riemann problem for (the scaled) system (1) and derive the characteristics $\lambda_1 = \sqrt{gH_0}, \lambda_2 = \ldots$ for (1) for the special case $H(x) = H_0$ constant.

   Rewrite (1) in vector form by using a matrix A, as follows (with $H_0 = H$):

   $$\partial_t \begin{pmatrix} \eta \\ H_0 u \end{pmatrix} + A\partial_x \begin{pmatrix} \eta \\ H_0 u \end{pmatrix} = 0 \tag{3}$$

   with appropriate 2×2 matrix A.

   Answer:

   $$A = \begin{pmatrix} 0 & 1 \\ c_0^2 & 0 \end{pmatrix} \tag{4}$$

with $c_0^2 = gH_0$. Find the eigenvalues λ and eigenvectors $\lambda_1 = c_0, \lambda_2 = -c_0$ of A, i.e. determine λ in $\det(A - \lambda I) = 0$ with identity matrix I. Construct the matrix of eigenvectors

$$B = \frac{1}{2c_0} \begin{pmatrix} 1 & -1 \\ c_0 & c_0 \end{pmatrix}. \tag{5}$$

Now $B^{-1}B = I$ and show that

$$B^{-1}AB = \begin{pmatrix} \lambda_1 & 0 \\ 0 & \lambda_2 \end{pmatrix} I. \tag{6}$$

By multiplying (3) (with the appropriate expression) and with $\mathbf{r} = B^{-1}(\eta, H_0 u)^T$ show that we obtain a decoupled set of linear advection equations

$$\partial_t \mathbf{r} + \begin{pmatrix} \lambda_1 & 0 \\ 0 & \lambda_2 \end{pmatrix} \partial_x \mathbf{r} = 0 \tag{7}$$

with $\mathbf{r} = (r_1, r_2)^T$ and $r_1 = H_0 u + c_0 \eta, r_2 = H_0 u - c_0 \eta$. By simple addition or subtraction of (1) (with one multiplication), show that we could immediately have arrived at these so-called Riemann invariants $\mathbf{r}$.

2. Now solve the Riemann problem of (7) for piecewise constant initial data

$$r_1(x,0) = \begin{cases} r_{1l} & \text{for } x < 0 \\ r_{1r} & \text{for } x \geq 0 \end{cases}, \quad r_2(x,0) = \begin{cases} r_{2l} & \text{for } x < 0 \\ r_{2r} & \text{for } x \geq 0 \end{cases}. \tag{8}$$

Show that the solution of this Riemann problem is (analyically and/or graphically –this may seem straightforward but please state the "obvious")

$$r_1(x,t) = \begin{cases} r_{1l} & \text{for } x < c_0 t \\ r_{1r} & \text{for } x \geq c_0 t \end{cases}, \quad r_2(x,t) = \begin{cases} r_{2l} & \text{for } x < -c_0 t \\ r_{2r} & \text{for } x \geq -c_0 t \end{cases}. \tag{9}$$

Using this solution solve the Riemann solution for (1), given that $r_1 = H_0 u + c_0 \eta, r_2 = H_0 u - c_0 \eta$ and $H_0 u = \frac{1}{2}(r_1 + r_2), \eta = \frac{1}{2}(r_1 - r_2)/c_0$, i.e., use the piecewise initial data u_l, u_r, η_l, η_r. Hence, show that

$$H_0 u(x,t) = \frac{1}{2}\left(r_1(x,t) + r_2(x,t)\right) = \begin{cases} H_0 u_l & \text{for } x < -c_0 t \\ \ldots & \text{for } -c_0 t \leq x \leq c_0 t \\ H_0 u_r & \text{for } x > c_0 t \end{cases}, \tag{10}$$

$$\eta(x,t) = \frac{1}{2}\left(r_1(x,t) - r_2(x,t)\right)/c_0 = \begin{cases} \eta_l & \text{for } x < -c_0 t \\ \ldots & \text{for } -c_0 t \leq x \leq c_0 t \\ \eta_r & \text{for } x > c_0 t \end{cases}. \tag{11}$$

Hence, we have defined the Riemann invariants $r_1 = H_0 u + \sqrt{(gH_0)}\eta, r_2 = \ldots$ of (1) (for this case with H_0 constant) and show that these are two uncoupled linear advection equations advected by the respective characteristics. By using this linear transformation from u, η to these new, Riemann variables r_1, r_2 and vice versa, solve the Riemann problem for the original system and in terms of the original variables.

3. Work out the Godunov scheme for (1) and derive a time step estimate. You can either use $(\eta, H_0 u)$ as variables but with an eye on the variable $H(x)$-case use (η, u) variables in the discretisation (simply relate these to r_1, r_2 where needed, i.e. in the flux only). Use extrapolating boundary conditions to mimic an "open" domain and use ghost values to mimic a closed domain by taking the velocity equal and opposite to the velocity in the domain while taking η to be equal on either side of te boundary. Alternatively, one may set the relevant flux to zero for solid walls at $x = 0, L$. (What should the condition on η be?) First consider the case with $H(x)$ constant, but extend the discretisation and code to variable but continuous $H(x)$. At each cell edge the Riemann solution/flux can be calculated with a "locally approximately constant" $H(x)$. Why is that reasonable?

4. *Numerics in Firedrake:* Implement the Godunov scheme for (1) in *Firedrake*[1] as zeroth-order discontinuous Galerkin method and verify it against standing wave solutions (derive/state these with solid wall boundary conditions –see theory lectures), or the exact Riemann solutions (derive/state these for open boundary conditions). Why is the finite volume scheme conservative? Plot various profiles (exact and numerical) in time from $3T_p$ to $4T_p$ with the relevant period T_p and, also for $9T_p$ to $10T_p$. (Visual convergence suffices but feel free to do a formal convergence analysis.) What should the order of accuracy be, in space and in time? Try various CFL-numbers including one, $\Delta t = \mathrm{CFL}\Delta x / \max \lambda$ with $0 \leq \mathrm{CFL} \leq 1$. Interpret your results. Do not use a counter but use actual dimensionless time in your time-loop.

5. Consider the finite volume scheme for (1), used in the previous question, i.e., before the numerical flux

[1] A Firedrake code for the symmetric flux of the last exercise has been supplied. In the symmetric flux a sympletic-Euler time scheme is used, while in the Godunov a forward-Euler time scheme is used. So change the time scheme, or check whether the (better?) symplectic-Euler time scheme does work with the Godunov scheme as well. A Firedrake code of a related wave problem provides an simpler introduction: `https://www.firedrakeproject.org/demos/linear_wave_equation.py.html`

was defined:

$$\bar{\eta}_k^{n+1} = \bar{\eta}_k^n - \frac{1}{\Delta x_k} \int_{t^n}^{t_{n+1}} (Hu)_{k+1/2} - (Hu)_{k-1/2} \, \mathrm{d}t \tag{12}$$

$$U_k^{n+1} = U_k^n - \frac{1}{\Delta x_k} \int_{t^n}^{t_{n+1}} (g\eta)_{k+1/2} - (g\eta)_{k-1/2} \, \mathrm{d}t \tag{13}$$

with flux $F_{\eta,k+1/2} \equiv (Hu)_{k+1/2} = H(x_{k+1/2})u(x_{k+1/2}, t)$ the exact function $H(x)$ times variable $u(x,t)$ and flux $F_{u,k+1/2} \equiv (g\eta)_{k+1/2} = g\eta(x_{k+1/2}, t)$ the constant g times variable η evaluated at the node $x_{k+1/2}$ separating the cells k and $k+1$, and cell averages U_k and $\bar{\eta}_k$ at their respective times t^n and t^{n+1}. Cell width $\Delta_k = x_{k+1/2} - x_{k-1/2}$. To close the scheme these two fluxes F_η and F_u at the cell faces or nodes need to be expressed in terms of the cell averages adjacent to this face. Instead of using the Godunov flux an alternating flux is used:

$$F_{\eta,k+1/2} = \theta H(x_{k+1/2}) U_{k+1}^n + (1-\theta) H(x_{k+1/2}) U_k^n \tag{14}$$

$$F_{\eta,k+1/2} = (1-\theta) g\bar{\eta}_{k+1}^{n+1} + \theta g \bar{\eta}_k^{n+1} \tag{15}$$

with $\theta \in [0,1]$ and while assuming that $H(x)$ is continuous[2]. The flux is alternating because the position of the weights θ and $(1-\theta)$ is reversed in the respective fluxes. In addition, we use the symplectic Euler time integrator which combines the forward and backward Euler schemes (see Morton and Mayers and the Internet). One can show that the alternating flux ensures that the discrete energy is conserved for infinitesimal time steps

$$E = \frac{1}{2} \sum_{k=1}^{N_{cells}} H_0 U_k^2 + g\bar{\eta}_k^2 \tag{16}$$

with N_{cells} the number of finite volumes/rods in the domain, but here it suffices to observe that the wave amplitude does not decay in time. For varying bottom topography or rest depth $H = H(x)$ this proof of energy conservation is more complicated.

6. Implement the solid-wall boundary conditions using that this flux at the boundary is zero. Be careful and take θ not close to 0 or 1 at the boundaries.

7. *Numerics in Firedrake:* Implement the scheme and test it against the exact standing wave or Riemann-problem solution. Monitor the energy as function of time with $H(x)$ in the middle of each cell replacing

[2]This flux has been implemented in the supplied code for the boundary conditions of the last exercise, with imposed influx and "extrapolating outflow". By changing the boundary conditions, initial condition, numerical fluxes, depth and domain size in this code or by using the code provided as reference for your own (improved) code, the various questions in this exercise can be addressed.

H_0 in (16). It is not required to make a convergence table but feel free to do so. Compare the two different flux schemes and give an interpretation.

8. The instructor from Seakayaking Cornwall posed the following question during the Advanced I Seakayaking Course. Given the offshore (mean or maximum) wave height in deep water A_d, in the absence of (massive) wave breaking, what is the wave height $A(x)$ in shallow water going to be before the start of the surf zone at the beach in which all waves start breaking? Since we are using (linear) shallow water theory one problem is that deep water waves effectively do not reach the bottom till the water reaches an intermediate depth $H_i = H_0$ where the wave amplitude is $A_i \approx A_d$ since for deep water the changes in topography are not changing the wave amplitude.

   For slowly varying bottom topography $H(x)$, it was shown, using an asymptotic theory for linear shallow water equations developed by Green but we refer instead to the recent article by Didulenkova et al. (2009), that the amplitude $A(x) < A_d$ behaves as follows

$$A(x) = A_d \left(\frac{H_0}{H(x)} \right)^{1/4} \tag{17}$$

   with $H(x) < H_0$ slowly varying in x towards the shoreline and H_0 an offshore depth . In addition, the frequency ω and wave number $k(x)$ satisfy the relation $\omega = \sqrt{gH(x)}k(x)$, implying that for waves of one frequency that the wave length $\lambda(x) = 2\pi/k(x)$ decreases when the depth $H(x)$ decreases twowards the shore. The combined effects mean that waves approaching the beach become shorter and higher, cf. mass and energy conservation.

   The goal is now to verify this asymptotic result (17) using a numerical code of the linear shallow water wave equations for the following varying bottom topography

$$H(x) = \begin{cases} H_0 & 0 < x < W \\ H_0 - s(x - W) & W \leq x \leq L_1 \\ H_b & L_1 < x < L \end{cases} \tag{18}$$

   with $W < L_1 < L$, $H_b < H_0$, $s = (H_0 - H_b)/(L_1 - W)$.

   We specify time-dependent data for incoming waves with, e.g., *dimensional* off-shore depth $H_{0s} =$ 40m, wave amplitude (half the wave height in wave forecasts) $A_d = 1$m, wave period $T = 6$s and horizontal scale $L_s = 225$m. Then, *now in dimensionless terms*, the velocity and total depth imposed via the boundary conditions at $x = 0$ are: $u_0(t) = C\sin(-\omega t)$, $C = gA_d k_w/\omega$, $k_w = \omega/\sqrt{gH_0}$ and $h(x \uparrow 0, t) = H_0 + \eta(0, t) = H_0 + A_d \sin(-\omega t)$ and $u(x \uparrow 0, t) = u_0(t)$. Take, e.g., *dimensionless* $W = 2, H_0 = 1, H_b = 0.1, L_1 = 10$ as well a suitable $L > L_1$. One can thus start from rest.

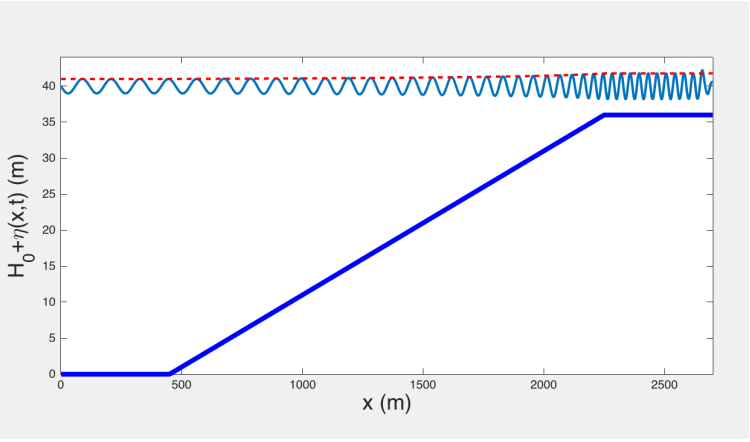

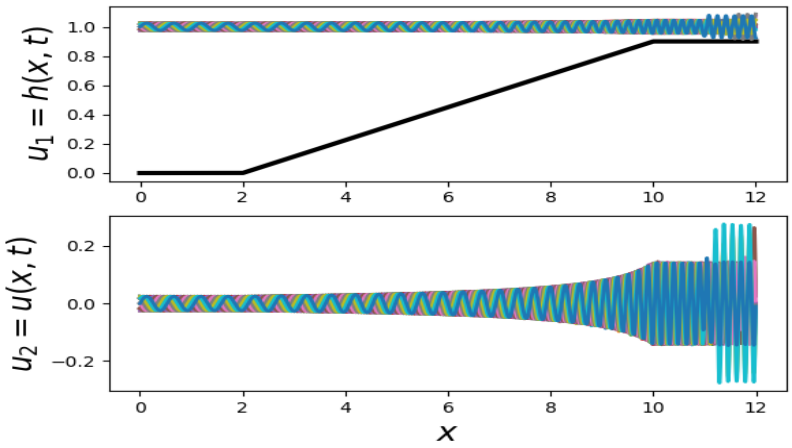

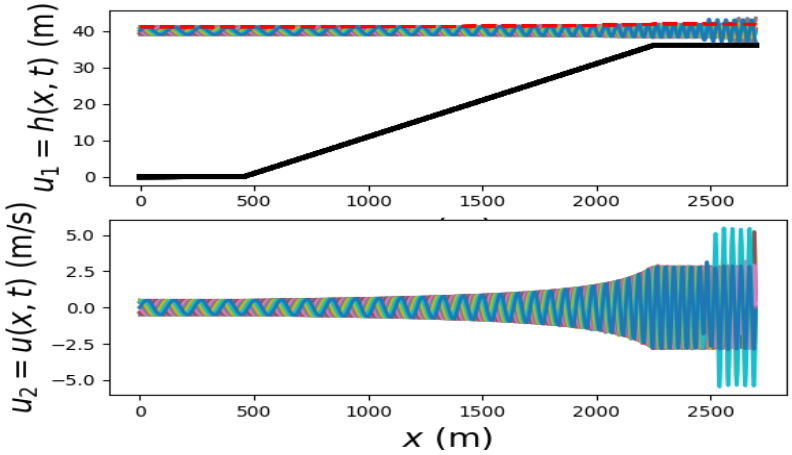

Figure 1: Sample snapshot(s) of a simulation results. Matlab simulation (dimensional display one snapshot) and Python simulation (dimensionless and dimensional displays). The provided Firedrake code for the symmetric flux yields similar results.

On the right, we take extrapolating boundary conditions, which is a poor condition, see Kristina (2014) for better outflow conditions. Simulate these waves for sufficiently a long time and with sufficient resolution to show that the wave amplification occurs when the water depth becomes shallower. A dimensionless end-time is $t = 41$ involving 45 wave periods.

Argue why, and implement if you wish, a nonuniform mesh is advantageous in this case. It may be advantageous to use the asymptotic result for the wavelength $\lambda(x) = 2\pi/k(x)$ in order to find a suitable non-uniform mesh.

Plot the maximum amplitude boundary $H_0 + A(x)$ and the topography as function of x towards the shore as well as a few intermediate time and final time profiles. Take a final time such that the effects of the (poor) outflow conditions are minimal but the waves' travel time is sufficiently long to draw conclusions. Display the answers/plots (also) in dimensional form even though the numerical integration will be dimensionless (by default). Perform the simulations and compare/plot the maximum amplitude with the above result (17) in plots, both dimensional and dimensionless plots of $u(x,t), h(x,t), \eta(x,t)$. Carefully verify that your results have converged numerically –a fair bit of resolution is required. Compare the results or both fluxes

Explore another case with steeper beach topography and draw your conclusions. Feel free to explore some more cases by varying the parameters[3].

Test both the symmetric (provided) and Godunov numerical fluxes.

9. (*Advanced/Optional:*) Extend the above exercises to the nonlinear shallow-water equations, meaning that (only) the numerical flux needs to be changed.

References

Ambati, V.R. and Bokhove, O. 2007: Space-time finite element shallow water flows. *J. Comp. Appl. Math.* **204**(2), 452–462.

Bercea, G.-T., McRae, A.T.T., Ham, D.A., Mitchell, L., Rathgeber, F., Nardi, L., Luporini, F., and Kelly, P.H.J. 2016: A structure-exploiting numbering algorithm for finite elements on extruded meshes, and its performance evaluation in Firedrake. *Geoscientific Model Development* **9**-10, 3803–3815.

Bokhove, O. (2023) Fluid Dynamics —Numerical Techniques. Reader.

[3]Do some tests in which the Godunov flux is compared with the symmetric flux.

I. Didulenkova, E. Pelinovsky, T. Soomere 2009: Long wave dynamics along a convex bottom. *J. Geophys. Res.* **114**. `https://agupubs.onlinelibrary.wiley.com/doi/epdf/10.1029/2008JC005027` The theory used is explained clearly and in an accessible way in the first few pages (3 to 7) of this article.

W. Kristina, B. van Groesen, and O. Bokhove 2012: Effective Coastal Boundary Conditions for Dispersive Tsunami Propagation. `https://ris.utwente.nl/ws/portalfiles/portal/5093369/memo1983.pdf`

Morton, K.W. and Mayers, D.F. (2005) *Numerical solution of partial differential equations.* Cambridge University Press, 227, 278 pp.

Internet.

W. Kristina (2014) *Effective coastal boundary conditions for tsunami simulations.* PhD Thesis, University of Twente. Section 2.3.1.

A Asymptotic solution of wave amplitude at the beach

The dimensional equations (1) can be rewritten into the following wave equation (after Didulenkova et al. (2009)):

$$\partial_{tt}\eta - \partial_x \left(c^2(x)\partial_x \eta\right) = 0 \tag{19}$$

with x-dependent $c^2(x) = gH(x)$. Substitution and evaluation of the Ansatz $\eta(x,t) = A(x)e^{i(\omega t - \Psi(x))}$ into (19), involving the unknown wave amplitude $A = A(x)$ and unknown (derivative of) wave number $k = k(x) = \mathrm{d}\Psi(x)/\mathrm{d}x$ and specified (incoming) wave frequency ω, yields

$$\left(\frac{\omega^2}{gH} - k^2\right) A + \frac{\mathrm{d}^2 A}{\mathrm{d}x^2} + \frac{1}{H}\frac{\mathrm{d}H}{\mathrm{d}x} A = 0 \tag{20a}$$

$$2k\frac{\mathrm{d}A}{\mathrm{d}x} + A\frac{\mathrm{d}k}{\mathrm{d}x} + \frac{1}{H}\frac{\mathrm{d}H}{\mathrm{d}x} Ak = 0 \tag{20b}$$

after splitting up real and imaginary parts. The second equation in (20) can be readily solved to give

$$A(x)^2 k(x) H(x) = A_d^2 k_0 H_0 \tag{21}$$

with offshore constant values of depth H_0, wave number k_0 and wave amplitude A_d as integration constants. When the topography $H(x)$ and wave amplitude $A(x)$ are slowly varying in space, then the first term in the first equation in (20) is approximately zero by itself such that

$$k^2 = \omega^2/(gH) \tag{22}$$

(approximation sign omitted). Hence, by combining (21) and (22), one finds the expression (17) stated in the main text, i.e. that

$$A(x)^4 H(x) = A_d^4 H_0. \tag{23}$$

B Firedrake Discontinuous Galerkin FEM: weak forms

A discontinuous Galerkin finite element method (DGFEM) is derived for the linear shallow-water equations with the use of an alternating numerical flux. Alternatively, as in the above, the Godunov flux can be implemented as well.

Consider the linear shallow-water system:

$$\partial_t \eta + \nabla \cdot (H(x)\mathbf{u}) = 0 \tag{24}$$

$$\partial_t \mathbf{u} + \nabla(g\eta) = 0. \tag{25}$$

In flux form, we have with $\mathbf{F}_\eta = H(x)\mathbf{u}, F_u = g\eta$ that

$$\partial_t \eta + \nabla \cdot (\mathbf{F}_\eta) = 0 \tag{26}$$

$$\partial_t \mathbf{u} + \nabla F_u = 0. \tag{27}$$

Multiply these equations by test functions w_η^K and $\mathbf{w}_u^K$ on each element K, respectively, and integrate by parts over each element K and sum over all elements. One obtains

$$\sum_K \int_K w_\eta \partial_t \eta - \mathbf{F}_\eta \cdot \nabla w_\eta \mathrm{d}x + \sum_K \int_{\partial K} w_\eta^l \hat{n}_l \cdot \mathbf{F}_\eta^l \mathrm{d}\Gamma = 0, \tag{28}$$

in which we will drop the integral signs hereafter as in Firedrake, used outward normal $\hat{n}$ and inside evaluation $(\cdot)^l$ on element K dubbed evaluation from the "left". Note that the sum over each face/node of an element can be transferred to a sum over all faces/nodes (cf. Ambati and Bokhove 2007), which then leads to two contributions: one from the inside of that element and from the adjacent element to that face

$$\sum_K w_\eta \hat{n} \cdot \mathbf{F}_\eta \mathrm{d}\Gamma = \sum_\Gamma \hat{n}_l \cdot \mathbf{F}_\eta^l w_\eta^l + \hat{n}_r \cdot \mathbf{F}_\eta^r w_\eta^r \, \mathrm{d}\Gamma \tag{29a}$$

$$= \sum_\Gamma (\alpha \mathbf{F}_\eta^l + \beta \mathbf{F}_\eta^r) \cdot (\hat{n}_l w_\eta^l + \hat{n}_r w_\eta^r) + (\hat{n}_l \mathbf{F}_\eta^l + \hat{n}_r \mathbf{F}_\eta^r)(\beta w_\eta^l + \alpha w_\eta^r) \, \mathrm{d}\Gamma \tag{29b}$$

$$= \sum_\Gamma (\alpha \mathbf{F}_\eta^l + \beta \mathbf{F}_\eta^r) \cdot (\hat{n}_l w_\eta^l + \hat{n}_r w_\eta^r) \, \mathrm{d}\Gamma \tag{29c}$$

$$\approx \sum_\Gamma \hat{n}^l \cdot \hat{\mathbf{F}}_\eta(U_l, U_r, \hat{n}_l)(w_\eta^l - w_\eta^r) \, \mathrm{d}\Gamma \tag{29d}$$

given that $\hat{n}^l = -\hat{n}^r$ and the flux is continuous $\mathbf{F}_\eta^l = \mathbf{F}_\eta^r$ such that $\hat{n}_l \mathbf{F}_\eta^l = \hat{n}_r \mathbf{F}_\eta^r$, weerein, $\alpha + \beta = 1$. Note that w_η^r is the test function on the element on the other side of the face/node. A numerical flux $\hat{\mathbf{F}}_\eta(U_l, U_r, \hat{n}_l$ replaces the linear combination of fluxes.

Hence, we obtain the weak formulation with in Firedrake the notation $\pm$ denoting left/right:

$$\begin{aligned}\sum_K w_\eta \partial_t \eta \mathrm{d}x = &\mathbf{F}_\eta \cdot \nabla w_\eta \mathrm{d}x - \sum_\Gamma \hat{n}^+ \cdot \hat{\mathbf{F}}_\eta(U_+, U_-, \hat{n}_+)(w_\eta^+ - w_\eta^-) \, \mathrm{d}S \\ &- \sum_\Gamma \hat{n}^+ \cdot \hat{\mathbf{F}}_\eta(U_+, U_-, \hat{n}_+) w_\eta^+ \, \mathrm{d}s(1) - \sum_\Gamma \hat{n}^+ \cdot \hat{\mathbf{F}}_\eta(U_+, U_-, \hat{n}_+) w_\eta^+ \, \mathrm{d}s(2),\end{aligned} \tag{30}$$

with boundary-types $\mathrm{d}s(1)$ and $\mathrm{d}s(2)$, interior faces $\mathrm{d}S$ and the vector of unknowns $U = (\eta, \mathbf{u})$. Likewise, for the velocity equation we obtain

$$\begin{aligned}\sum_K \mathbf{w}_u \cdot \partial_t \mathbf{u} =& F_u \nabla \cdot \mathbf{w}_u \mathrm{d}x - \sum_\Gamma \hat{F}_u(U_+, U_-, \hat{n}_+)\hat{n}^+ \cdot (\mathbf{w}_u^+ - \mathbf{w}_u^-)\,\mathrm{d}S \\ &- \sum_\Gamma \hat{F}_u(U_+, U_-, \hat{n}_+)\hat{n}^+ \cdot \mathbf{w}_u^+\,\mathrm{d}s(1) - \sum_\Gamma \hat{F}_u(U_+, U_-, \hat{n}_+)\hat{n}^+ \cdot \mathbf{w}_u^+\,\mathrm{d}s(2). \end{aligned} \tag{31}$$

An alternating numerical flux is used

$$\hat{\mathbf{F}}_\eta(U_+, U_-, \hat{n}_+) = \theta H(x)\mathbf{u}^+ + (1-\theta)H(x)\mathbf{u}^+ \tag{32a}$$

$$\hat{F}_u(U_+, U_-, \hat{n}_+) = (1-\theta)g\eta^+ + \theta g \eta^-, \tag{32b}$$

recalling that $H(x)$ is taken to be continuous, which leads to energy conservation under suitable boundary conditions. A leading-order of finite volume approach arises when the test functions are taken unity or zero in each element. For zeroth-order DGFEM or finite volume, the interior integrals with the gradients on the test function of course disappear in the above weak forms.

For the numerical implementation, we used the above weak forms and the DGFEM examples at `https://www.firedrakeproject.org/documentation.html`.

B.1 Numerics of boundary conditions

The boundary conditions are incorporated by specification of the ghost "right"- or $-$-value in the numerical flux. For solid walls, $\eta^l = \eta^r$ and $\hat{n}^l \cdot \mathbf{u}^l = \hat{n}^r \cdot \mathbf{u}^r$ or $\hat{n}^l \cdot \mathbf{u}^l = \hat{n}^l \cdot \mathbf{u}^r$. Inward coming waves at $x = 0$ can be specified by using a linear travelling-wave solution for η^r and $\hat{n}^l \cdot \mathbf{u}^r$. For outflow an extrapolting boundary condition is used by copying over the interior value, which yields some reflection. See Kristina et al. (2012) for better outflow conditions.

Exercise: (a) Implement the Godunov-flux into the Firedrake code and test. (b) Consider the outflow boundary condition in Kristina et al. (2012), implement it into the codes and test. (c) Consider the extruded-mesh strategy for one element of Bercea et al. (2016) and use it to establish a faster code. (d) Make a comparison between the codes, make the Firedrake code faster and test. (e) Extend the Firedrake code to higher-order DGFEM, by adding the interior integrals and also consider using other solver parameters since the mass matrix will no longer be diagonal. Test. All tests should include higher-resolution runs in space and time; it may therefore be best to consider one set of profiles at a late time.